Spatial Aliasing Artifacts Produced by Linear and Circular Loudspeaker Arrays used for Wave Field Synthesis

Sascha Spors[1] and Rudolf Rabenstein[2]

[1] *Deutsche Telekom Laboratories, Ernst-Reuter Platz 7, 10587 Berlin, Germany*

[2] *Telecommunications Laboratory, University Erlangen-Nuremberg, Cauerstrasse 7, 91058 Erlangen, Germany*

Correspondence should be addressed to Sascha Spors (`Sascha.Spors@telekom.de`)

ABSTRACT

Wave field synthesis allows the exact reproduction of sound fields if the requirements of its physical foundation are met. However, the practical realization imposes certain technical constraints. One of these is the application of loudspeaker arrays as an approximation to a spatially continuous source distribution. The effect of a finite spacing of the loudspeakers can be described as spatial sampling artifacts. This contribution derives a description of the spatial sampling process for planar linear and circular arrays, analyzes the sampling artifacts and discusses the conditions for preventing spatial aliasing. It furthermore introduces the reproduced aliasing-to-signal ratio as a measure for the energy of aliasing contributions.

1. INTRODUCTION

Wave field synthesis is one of the key technologies for spatial sound reproduction. Based on a purely physical description of acoustic wave fields, it has the potential for an exact reproduction of desired sound fields within an extended listening area. The effect of virtual sound sources (primary sources) is recreated by a continuous distribution of monopole and dipole sources on a closed surface around the listening area (secondary sources). However, in practical installations it is necessary to deviate from the strict requirements of the physical principles. For technical reasons, the continuous distribution of secondary sources is replaced by an arrangement of loudspeakers at discrete positions. This approximation can be described as a spatial sampling process, which potentially creates spatial aliasing artifacts. These artifacts may not only impair the perceived audio reproduction quality, they can also affect the application of active control techniques.

For the perceived reproduction quality spatial aliasing plays no dominant role since the human auditory system doesn't seem to be too sensible for spatial aliasing. A distance of 10...30 cm between the loudspeakers has proven to be suitable in practice for reproduction only purposes [3, 4]. However, the underlying psychoacoustic mechanisms are not clear and there are implications that spatial aliasing produces colorations of the perceived sound [5]. Hence, a detailed mathematical analysis of spatial aliasing artifacts may help to understand the psychoacoustic mechanisms on the one hand, and on the other hand to improve reproduction quality.

The performance of active control applications like active listening room compensation [6], active noise control (ANC) and acoustic echo cancelation (AEC) will be limited by spatial aliasing. A detailed analysis of spatial aliasing artifacts helps to predict the performance of such techniques.

Sampling conditions for wave fields have already been investigated e.g. by [1, 2]. However, the requirements for wave field reproduction have not been considered. Typical implementations of WFS systems are based on (piecewise) linear or circular shaped loudspeaker arrays. An anti-aliasing condition for linear loudspeaker arrays has already been published [4, 7]. However, to the knowledge of the authors no detailed analysis of the aliasing artifacts for linear neither for circular arrays has been performed so far. This paper analyzes the spatial aliasing artifacts of linear and circular loudspeaker arrays used for sound reproduction. Based on this analysis, anti-aliasing conditions are derived.

The frequency domain description of time domain sampled signals, by way of their Fourier transformation, has proven to be a powerful tool in the past for the description of temporal aliasing. A similar approach is chosen in this paper by interpreting acoustic wave fields as multidimensional signals.

The paper is organized as follows: A mathematical description of the wave field produced by an arbitrary shaped contour of secondary sources is presented in Section 2. It is shown that the reproduced wave field can be derived by a generalized spatio-temporal convolution (filtering) of the secondary source driving signal with the wave field produced by a secondary source. At first, the geometry is specialized to linear arrays in Section 3. Then similar steps as for a linear array are performed for the

analysis of circular arrays in Section 4. Section 5 illustrates the application of the derived sampling theorems to point sources as secondary sources, and finally Section 6 gives a summary and conclusion.

1.1. Nomenclature

The following conventions are used in this paper: For scalar variables lower case denotes the time domain, upper case the temporal frequency domain. Vectors are denoted by lower case boldface. The spatial frequency domain is denoted by a tilde placed over the respective symbol. The coordinate system in which a quantity is defined is denoted by the symbols C or P in the index of a quantity, where C denotes the Cartesian coordinate system and P the polar coordinate system. The two-dimensional position vector in Cartesian coordinates is given as $\mathbf{x_C} = [x\ y]^T$ and in polar coordinates as $\mathbf{x_P} = [\alpha\ r]^T$, where $x = r\cos\alpha$ and $y = r\sin\alpha$.

2. SOUND REPRODUCTION

The following section briefly reviews the foundations of sound reproduction systems and the concept of wave field synthesis.

2.1. Fundamentals of Sound Reproduction

The theoretical basis of sound reproduction is given by the Kirchhoff-Helmholtz integral [8]

$$P(\mathbf{x},\omega) = -\oint_{\partial V} \left(G(\mathbf{x}|\mathbf{x}_0,\omega)\frac{\partial}{\partial \mathbf{n}}S(\mathbf{x}_0,\omega) - \right.$$
$$\left. -S(\mathbf{x}_0,\omega)\frac{\partial}{\partial \mathbf{n}}G(\mathbf{x}|\mathbf{x}_0,\omega) \right)\ dS_0\ , \quad (1)$$

where $G(\mathbf{x}|\mathbf{x}_0,\omega)$ denotes a suitable chosen free-field Green's function, $\partial/\partial\mathbf{n}$ the directional gradient, $\mathbf{x}$ a point in the closed region V ($\mathbf{x} \in V$) and $\mathbf{x}_0$ a point on the boundary ∂V of that region. The underlying geometry is illustrated in Figure 1. Please note, that the region V may be two- or three-dimensional. In the first case V describes a plane and ∂V the closed contour surrounding it, in the second case V describes a volume and ∂V the closed surface surrounding it.

The free-field Green's function $G(\mathbf{x}|\mathbf{x}_0,\omega)$ can be interpreted as the field of a monopole source placed at the point $\mathbf{x}_0$. The directional gradient of typical free-field Green's functions used in this context can be interpreted as the field of a dipole source placed at $\mathbf{x}_0$, whose main axis lies in direction of the
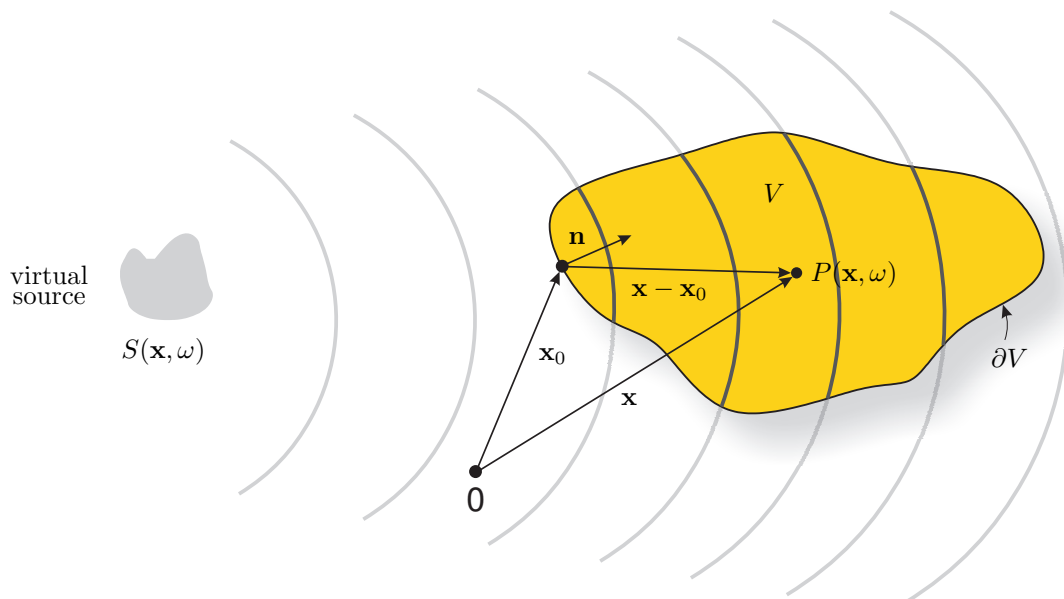
Fig. 1: Parameters used for the Kirchhoff-Helmholtz integral (1).

normal vector $\mathbf{n}$. Hence the Kirchhoff-Helmholtz integral states, that the acoustic pressure inside the region V can be controlled by a monopole and a dipole source distribution on the boundary ∂V enclosing the region V. These sources are termed as secondary sources in the following. The field outside of V is zero.

In practice it is desirable to utilize only one of the two secondary source types. The second term in the Kirchhoff-Helmholtz integral (1) involving the dipole sources can be eliminated under the following assumptions [9, 10, 11]:

1. excitation of only those secondary sources where the normal vector $\mathbf{n}$ has a component in the direction of the local propagation direction of the virtual source wave field,

2. limitation to concave secondary source contours ∂V, and

3. doubling of the strength of the driving function in order to cope for the elimination of the dipole sources.

A consequence of using monopoles only for sound reproduction is that the field outside the area V will not vanish any more.

The reproduced wave field for monopole-only reproduction is given as follows [10, 11]

$$P(\mathbf{x},\omega) = \\ -\oint_{\partial V} \underbrace{2a(\mathbf{x_0})\frac{\partial}{\partial \mathbf{n}}S(\mathbf{x_0},\omega)}_{D(\mathbf{x}_0,\omega)}\, G(\mathbf{x}|\mathbf{x_0},\omega)\, dS_0\ , \quad (2)$$

where $D(\mathbf{x}_0,\omega)$ denotes the secondary source driving function and $a(\mathbf{x_0})$ a window function which takes care that only the relevant secondary sources are excited (see first assumption made above). The free-field Green's function $G(\mathbf{x}|\mathbf{x_0},\omega)$ used in Eq. (2) has not been specified so far. The next two sections specialize the Green's function to three- and two-dimensional sound reproduction scenarios.

2.2. Three-Dimensional Sound Reproduction

The particular form of the Green's function depends on the dimensionality of the problem and the homogeneous boundary conditions imposed on ∂V. For sound reproduction free-field conditions are desired. Hence, the three-dimensional free-field Green's function is the appropriate choice for three-dimensional

sound reproduction. It is given as follows [8]

$$G_{3\mathrm{D}}(\mathbf{x}|\mathbf{x}_0,\omega) = \frac{1}{4\pi}\frac{e^{-jk|\mathbf{x}-\mathbf{x}_0|}}{|\mathbf{x}-\mathbf{x}_0|}. \qquad (3)$$

Equation (3) can be interpreted as the field of a monopole point source located at the position $\mathbf{x}_0$.

In the remainder of this paper, the spatial Fourier transformation of the three-dimensional free-field Green's function is required. The spatial Fourier transformation $\tilde{G}_{\mathrm{c,3D}}(\mathbf{k}_\mathrm{c},\omega)$ of $G_{3\mathrm{D}}(\mathbf{x}|\mathbf{0},\omega)$ can be calculated by way of its Hankel transformation. It is given as [12]

$$\tilde{G}_{\mathrm{c,3D}}(\mathbf{k}_\mathrm{c},\omega) = \frac{1}{4\pi}\frac{1}{\sqrt{k_x^2+k_y^2-(\frac{\omega}{c})^2}}\ . \qquad (4)$$

2.3. Two-Dimensional Sound Reproduction

In general, it will not be feasible to control the pressure on the entire two-dimensional surface of a three-dimensional volume. Typical reproduction systems are therefore restricted to the reproduction in a plane only.

The required reduction in dimensionality is performed by assuming that the reproduced wave field is independent from the z-coordinate, e. g. $P_\mathrm{c}(x,y,z,\omega) = P_\mathrm{c}(x,y,\omega)$. The two-dimensional free-field Green's function is given as [8]

$$G_{2\mathrm{D}}(\mathbf{x}|\mathbf{x}_0,\omega) = \frac{j}{4}H_0^{(2)}(k\,|\mathbf{x}-\mathbf{x}_0|)\ , \qquad (5)$$

where $H_\nu^{(1),(2)}(\cdot)$ denotes the ν-th order Hankel function of first/second kind [13]. Equation (5) can be interpreted as the field of a monopole line source which intersects the reproduction plane at the position $\mathbf{x}_0$.

The spatial Fourier transformation of $G_{2\mathrm{D}}(\mathbf{x}|\mathbf{0},\omega)$ can be calculated by way of its Hankel transformation. It is given as

$$\tilde{G}_{\mathrm{c,2D}}(\mathbf{k}_\mathrm{c},\omega) = -\frac{1}{4(k_x^2+k_y^2-(\frac{\omega}{c})^2)}+$$
$$+\frac{j}{4\sqrt{k_x^2+k_y^2}}\delta(\sqrt{k_x^2+k_y^2}-\frac{\omega}{c})\ . \quad (6)$$

The discussion of aliasing artifacts in the remainder of this paper will be limited to reproduction systems that aim at the reproduction of the virtual source wave field in a plane only.

2.4. Wave Field Synthesis

The theory of sound reproduction, as presented so far, assumed that a two-dimensional sound reproduction system is realized with monopole line sources as secondary sources. The concept of wave field synthesis (WFS) however, utilizes point sources as secondary sources [4, 14, 15, 16, 17, 18]. A reason for this choice is that closed loudspeakers constitute reasonable approximations of point sources. A WFS system is typically realized by using loudspeaker arrays located in a plane which surround the listening area. These loudspeakers should be leveled with the listeners ears for best results. The listening area and the surrounding loudspeaker array may have arbitrary shapes.

Choosing point sources instead of line sources leads to spectral and amplitude artifacts being present in the reproduced wave field. These artifacts can be corrected to some extend by modifying the driving function $D(\mathbf{x}_0,\omega)$. The artifacts of WFS have been discussed in detail by [17, 18, 19]. It is assumed in the following, that line sources are used for two-dimensional sound reproduction. However, the derived results can be applied straightforward to point sources as secondary sources. This is shown in Section 5.

2.5. Frequency Domain Representation of the Reproduced Wave Field

The free-field Green's functions given by Eq. (3) and Eq. (5) do not explicitly depend on the points $\mathbf{x}$ and $\mathbf{x}_0$, but on their distance $G(\mathbf{x}|\mathbf{x}_0,\omega) = G(\mathbf{x}-\mathbf{x}_0,\omega)$. Hence, for free-field propagation Eq. (2) can be interpreted as a generalized convolution integral. The driving function $D(\mathbf{x}_0,\omega)$ is convolved with the secondary source field $G(\mathbf{x}-\mathbf{x}_0,\omega)$. The convolution is performed on/along the closed surface/contour ∂V. The convolution of two time-domain signals is conveniently represented in the temporal frequency domain by using the convolution theorem of the Fourier transformation. Furthermore the frequency domain description of time-domain sampled signals is very efficient to describe aliasing artifacts. This suggest that a spatio-temporal frequency-domain description of the reproduced wave field $P(\mathbf{x},\omega)$ is useful in order to describe the reproduced wave field for a discrete secondary source distribution. However, for

the generalized convolution (2) this desired description cannot be derived straightforward for arbitrary secondary source contours.

This paper concentrates therefore on the derivation of the spatial aliasing artifacts for two specific geometries: on linear and on circular secondary source contours ∂V. The next section discusses the sampling artifacts of linear arrays, Section 4 the artifacts of circular arrays.

3. SAMPLING ARTIFACTS PRODUCED BY LINEAR ARRAYS

A detailed analysis of the sampling artifacts produced by linear loudspeaker arrays has already been published by one of the authors in [20]. This section provides an overview of the results.

3.1. Reproduced Wave Field

Without loss of generality, the geometry depicted in Fig. 2 is assumed: a linear secondary source distribution which is located on the x-axis ($y = 0$) of a Cartesian coordinate system. The reproduced wave field is derived from Eq. (2) by degenerating the closed contour ∂V to a line with infinite length. This line will divide the x-y-plane into two-regions. One of these can be chosen as the listening area. The upper half plane ($y > 0$) is used as listening area in the following. Please note that in the listening area only those virtual source wave fields can be reproduced where the local propagation direction at the secondary source distribution has a component in the direction of the normal vector $\mathbf{n}$.

Specializing Eq. (2) to the geometry depicted by Fig. 2 yields

$$P_{\mathsf{C}}(\mathbf{x}_{\mathsf{C}}, \omega) =$$
$$- \int_{-\infty}^{\infty} D_{\mathsf{C}}(\mathbf{x}_{\mathsf{C},0}, \omega) \, G_{\mathsf{C},2\mathrm{D}}(\mathbf{x}_{\mathsf{C}} - \mathbf{x}_{\mathsf{C},0}, \omega) \, dx_0 \ , \quad (7)$$

where $\mathbf{x}_{\mathsf{C},0} = [\ x_0 \ \ 0 \ ]^T$. Applying a two-dimensional spatial Fourier transformation [8] to Eq. (7) yields the pressure field in the spatio-temporal frequency domain as

$$\tilde{P}_{\mathsf{C}}(\mathbf{k}, \omega) = -\tilde{D}_{\mathsf{C}}(k_x, \omega) \, \tilde{G}_{\mathsf{C},2\mathrm{D}}(\mathbf{k}_{\mathsf{C}}, \omega) \ . \qquad (8)$$

The vector $\mathbf{k}_{\mathsf{C}} = [\ k_x \ \ k_y \ ]^T$ denotes the spatial frequency vector (wave vector), where for acoustic wave fields $|\mathbf{k}| = \omega/c$.

In order to derive the effects of spatial sampling and

a sampling theorem, the spatio-temporal spectrums of the secondary sources $\tilde{G}_{\mathsf{C},2\mathrm{D}}(\mathbf{k}_{\mathsf{C}}, \omega)$ and the driving function $\tilde{D}_{\mathsf{C}}(k_x, \omega)$ have to be considered. The spectrum of the driving function $\tilde{D}_{\mathsf{C}}(k_x, \omega)$ depends on the wave field of the virtual source $S_{\mathsf{C}}(\mathbf{x}_{\mathsf{C}}, \omega)$. It is sufficient to consider a plane wave as wave field for the virtual source, since arbitrary wave fields can be decomposed into plane waves [8].

3.2. Sampling Artifacts for the Reproduction of Plane Waves

For the upper half plane ($y > 0$), the secondary source distribution is only capable of reproducing plane waves traveling into the positive y-direction. It is therefore reasonable to limit the incidence angle of the virtual plane waves to $0 \leq \alpha_{\mathrm{pw}} < \pi$ in the following. The reproduced wave field $\tilde{P}_{\mathsf{C},S,\mathrm{pw}}(\mathbf{k}, \omega)$ for a spatially discrete secondary source distribution is given as [20]

$$\tilde{P}_{\mathsf{C},S,\mathrm{pw}}(\mathbf{k}, \omega) =$$
$$\pi \frac{\omega}{c} \sin \alpha_{\mathrm{pw}} \sum_{\eta=-\infty}^{\infty} \delta(k_x - \frac{2\pi}{\Delta x}\eta - \frac{\omega}{c} \cos \alpha_{\mathrm{pw}}) \times$$
$$\times \left(\frac{1}{k} \delta(\sqrt{k_x^2 + k_y^2} - \frac{\omega}{c}) + j \frac{1}{k_x^2 + k_y^2 - (\frac{\omega}{c})^2} \right) \ . \tag{9}$$

The reproduced spectrum consists of a real and an imaginary part. The imaginary part can be identified as being produced by the near-field of the secondary sources. This part is neglected first for the derivation of the sampling artifacts. For a fixed temporal frequency ω, the first Delta function in the real part of Eq. (9) can be interpreted as a series of Dirac lines perpendicular to the k_y-axis at the positions $k_x = \frac{2\pi}{\Delta x}\eta + \frac{\omega}{c} \cos \alpha_{\mathrm{pw}}$. The second Delta function can be interpreted as a circular Dirac pulse with the radius $\frac{\omega}{c}$. Figure 3 illustrates the real part of $\tilde{P}_{\mathsf{C},S,\mathrm{pw}}$ in the spatial k_x-k_y-frequency plane. Due to the sifting property of Dirac functions, the result of the multiplication of the two Dirac functions is given by their intersections in the spatial frequency plane. The result for $\eta = 0$ comprises the desired plane wave. The other terms in the sum for $\eta \neq 0$ are potential aliasing contributions.

For the situation shown in Fig. 3, the result are two Dirac pulses at the positions indicated by the dots •. In this particular example, these two represent the
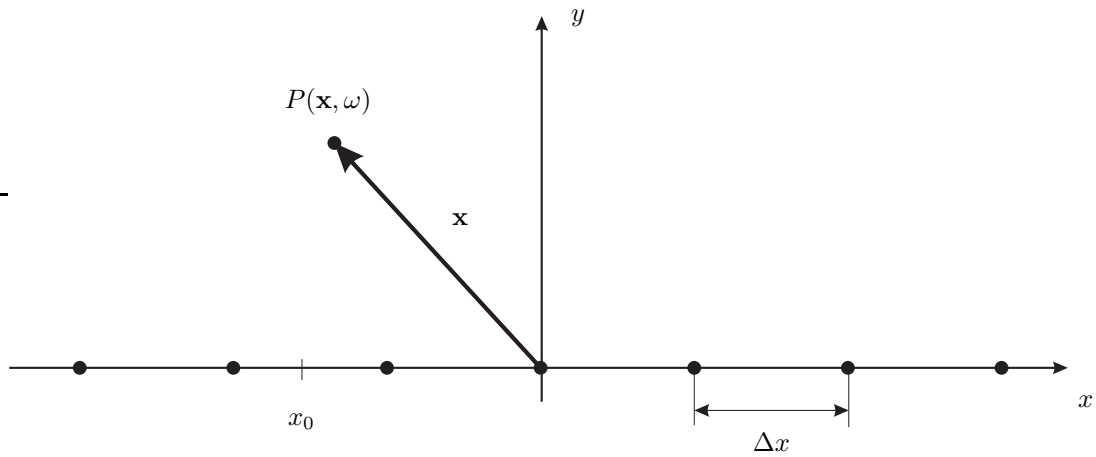
Fig. 2: Geometry used to derive the sampling artifacts of linear loudspeaker arrays. The $\bullet$ denote the sampling positions of the secondary sources and the gray plane the reproduction area for a plane wave with incidence angle α_{pw} using a finite length array.
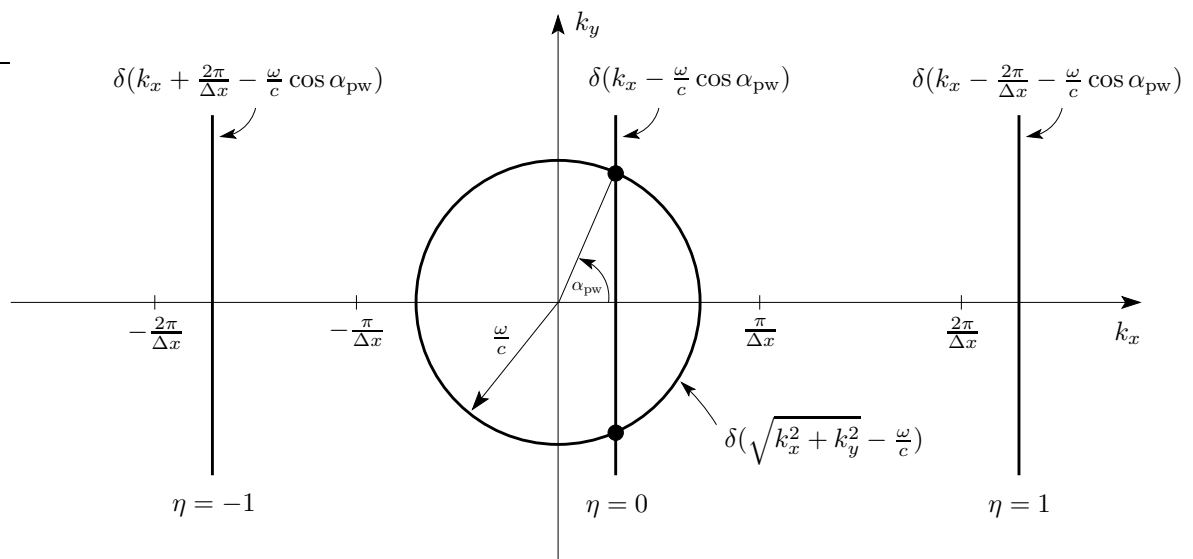

Fig. 3: Illustration of the real part of the spectrum $\tilde{P}_S$ reproduced by a discrete secondary monopole source distribution for the reproduction of a plane wave with incidence angle α_{pw}. The resulting spectrum is given by the intersection of the two Dirac functions at the positions indicated by the dots $\bullet$.

desired wave field of a plane wave traveling into the positive y-direction for the upper half plane ($y > 0$) and into the negative y-direction for the lower half plane ($y < 0$). This symmetry results from the reproduction using secondary monopole sources only. For an increasing distance Δx between the secondary sources or an increasing frequency $\omega = 2\pi f$ there may also be additional contributions besides the desired plane wave in the reproduced wave field. In this first case, the repetitions of the Dirac lines in the real part of Eq. (9) for $\eta \neq 0$ move towards the circular Delta function. In the second case, the radius of the circular Dirac pulse increases and the Dirac lines move towards higher values of k_x. If more than one Dirac line overlaps with the circular Delta function additional plane wave contributions result. These contributions constitute spatial aliasing due to spatial sampling of the secondary source distribution. They are avoided if the frequency of the reproduced plane wave is limited. An anti-aliasing condition for the driving function can be derived from Fig. 3 and Eq. (9) as

$$ f \leq \frac{c}{\Delta x \left(1 + |\cos \alpha_{\mathrm{pw}}|\right)} \; . \qquad (10) $$

Thus, a reduction of the temporal frequency and/or the incidence angle of the reproduced monochromatic plane wave avoids spatial aliasing present in the reproduced wave field. Please note that the condition (10) differs from the one derived in [4] since the propagation characteristics of the secondary sources are included.

If the anti-aliasing condition (10) is not fulfilled, aliasing artifacts are present in the reproduced wave field. According to Fig. 3 and Eq. (9) these artifacts constitute a superposition of plane waves with different incidence angles than the desired plane wave. So far, only the real part of the reproduced spectrum was considered. The anti-aliasing condition (10) applies only approximately to the imaginary part of the reproduced spectrum. This is due to the fact that the part of the secondary source spectrum belonging to the evanescent contributions of the reproduced wave field is not strictly band-limited. However, its singular value and hence its main contribution to the reproduced wave field is located on the circular contour shown in Fig. 3.

Up to now, the linear secondary source distribution was assumed to be of infinite length in the

x-direction. However, practical implementations of linear loudspeaker arrays will always be of finite length. For the reproduction of plane waves, the effect of truncation can be approximated quite well by simple geometric means, as illustrated by the gray area in Fig. 2. This approximation states that a plane wave will be reproduced only in a tilted rectangular area in front of the array, whose width is equivalent to the aperture of the array in the x-direction and whose length in the y-direction is infinite. The area is tilted by the incidence angle α_{pw} of the plane wave to be reproduced.

As a consequence to this limited reproduction area, the aliasing effects discussed above depend on the listener position. This is due to the fact, that not all plane waves are reproduced at all listener positions. A special case is represented by a plane wave with an incidence angle of $\alpha_{\mathrm{pw}} = 90°$ and listener positions far away from the array: no aliasing artifacts will be present here. The aliasing frequency is infinite in this case.

3.3. Application Example

In the following example the reproduction of a monochromatic plane wave with an incidence angle of $\alpha_{\mathrm{pw}} = 90°$ and a frequency of $f_0 = 10$ kHz using a linear discrete distribution of secondary line sources is considered. The sampling distance between the secondary sources is chosen to $\Delta x = 0.15$m. Figure 4 illustrates the incidence angles of the reproduced plane waves in a polar diagram. Each line represents a plane wave traveling into the depicted direction. The dashed line represents the desired plane wave, the solid lines the aliasing contributions. Besides the desired plane wave, eight plane waves constituting aliasing are reproduced in this particular example.

The gray wedge shown in Fig. 4 illustrates the effect of truncation for an array with a total length of $l = 2.10$ m and a listener position in the center of the array ($x_l = 0$ m) at a distance of $y_l = 1$ m. Only plane wave contributions within the angles depicted by the gray wedge are reproduced.

4. SAMPLING ARTIFACTS PRODUCED BY CIRCULAR ARRAYS

The following section discusses the sampling artifacts produced by circular loudspeaker arrays. It is convenient to use polar coordinates for the description of the reproduced wave field in this case due to
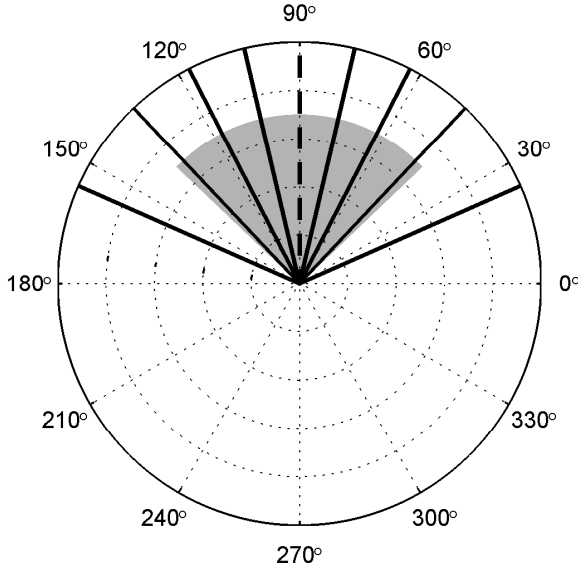
Fig. 4: Incidence angle of the desired plane wave α_{pw} (dashed line) and its aliasing contributions $\alpha_{\mathrm{pw},\eta_{\mathrm{al}}}$ (solid lines). The gray wedge illustrates the effect of truncation for one particular listener position.

the underlying circular geometry of the problem.

4.1. Reproduced Wave Field

In the following the wave field reproduced by a circular shaped discrete secondary source distribution with radius R is investigated. Figure 5 illustrates the geometry. The reproduced wave field $P_{\mathrm{P}}(\mathbf{x}_{\mathrm{P}},\omega)$ is given by specializing Eq. (2) to the geometry depicted in Fig. 5

$$P_{\mathrm{P}}(\mathbf{x}_{\mathrm{P}},\omega) = -\frac{j}{4}\int_0^{2\pi} D_{\mathrm{P}}(\alpha_0,R,\omega)\, H_0^{(2)}(k\Delta r)\, R\, d\alpha_0 \,,$$

(11)

where $\Delta r = |\mathbf{x}_{\mathrm{P}} - \mathbf{x}_{\mathrm{P},0}|$. The Hankel function $H_0^{(2)}(k\Delta r)$ in Eq. (11) can be expressed by Bessel and Hankel functions which depend only on one of the positions $\mathbf{x}_{\mathrm{P}}$ and $\mathbf{x}_{\mathrm{P},0}$ using the shift theorem of the Hankel functions. For $r \leq R$ the Hankel function $H_0^{(2)}(k\Delta r)$ can be expressed as follows [8]

$$H_0^{(2)}(k\,|\mathbf{x}_{\mathrm{P}} - \mathbf{x}_{\mathrm{P},0}|) =$$
$$\sum_{\nu=-\infty}^{\infty} J_\nu(kr) H_\nu^{(2)}(kR) e^{j\nu(\alpha-\alpha_0)} \,. \quad (12)$$

Introducing Eq. (12) into Eq. (11) yields the repro-

duced wave field inside the circular boundary ∂V as

$$P_{\mathrm{P}}(\mathbf{x}_{\mathrm{P}},\omega) = -\frac{j}{4}\sum_{\nu=-\infty}^{\infty} J_\nu(kr)\, H_\nu^{(2)}(kR)\, R\, e^{j\nu\alpha} \times$$

$$\times \int_0^{2\pi} D_{\mathrm{P}}(\alpha_0,R,\omega)\, e^{-j\nu\alpha_0}\, d\alpha_0 =$$

$$= -j\frac{\pi}{2}R \sum_{\nu=-\infty}^{\infty} J_\nu(kr)\, H_\nu^{(2)}(kR)\, \mathring{D}(\nu,R,\omega)\, e^{j\nu\alpha} \,,$$

(13)

where for the second equality the definition of the Fourier series [21] was used to eliminate the angular integral. Equation (13) states that the reproduced wave field is given by a Fourier series with respect to the angle α. The coefficients of this series are given by the Fourier series coefficients $\mathring{D}(\nu,R,\omega)$ of the driving function weighted by a Bessel and a Hankel function.

The effect of discretizing the secondary source distribution is modeled by sampling the loudspeaker driving function $D_{\mathrm{P}}(\alpha_0,R,\omega)$ at equidistant angles, resulting in a total of N sampled secondary source positions. The sampled driving function $D_{\mathrm{P,S}}(\alpha_0,R,\omega)$ is given as

$$D_{\mathrm{P,S}}(\alpha_0,R,\omega) = D_{\mathrm{P}}(\alpha_0,R,\omega) \sum_{\phi=0}^{M-1} \delta(\alpha_0 - \frac{\phi}{M}2\pi) \,.$$

(14)

Angular sampling results in repetitions of the angular spectrum. Applying this principle to the sampled driving function $D_{\mathrm{P,S}}(\alpha_0,R,\omega)$ results in the Fourier series coefficients $\mathring{D}_{\mathrm{S}}(\nu,R,\omega)$ of the sampled driving function

$$\mathring{D}_{\mathrm{S}}(\nu,R,\omega) = \sum_{\eta=-\infty}^{\infty} \mathring{D}(\nu+\eta N,R,\omega) \,. \qquad (15)$$

Introducing Eq. (15) into Eq. (13) yields the wave field $P_{\mathrm{P,S}}(\mathbf{x}_{\mathrm{P}},\omega)$ reproduced by a discrete secondary source distribution as

$$P_{\mathrm{P,S}}(\mathbf{x}_{\mathrm{P}},\omega) = -j\frac{\pi}{2}R \sum_{\eta=-\infty}^{\infty} \sum_{\nu=-\infty}^{\infty} \times$$

$$\times J_\nu(kr)\, H_\nu^{(2)}(kR)\, \mathring{D}_{\mathrm{S}}(\nu+\eta N,R,\omega)\, e^{j\nu\alpha} \,. \quad (16)$$

The result for $\eta = 0$ constitutes the desired wave field. Please note, that effects of the limited aperture of the array are included inherently in Eq. (16)
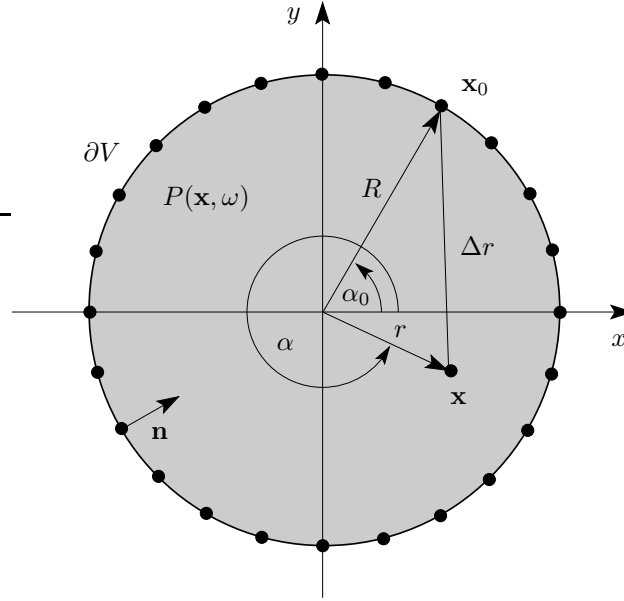
Fig. 5: Geometry used to derive the sampling artifacts of circular loudspeaker arrays. The dots • denote the spatial sampling positions of the driving function $D_{\mathrm{P}}(\alpha_0, R, \omega)$.

by the Hankel function $H_\nu^{(2)}(kR)$. The terms for $\eta \neq 0$ are potential aliasing contributions.

Equation (15) and (16) imply that the bandwidth of $\mathring{D}(\nu, R, \omega)$ in the angular frequency domain has to be limited in order to avoid spatial aliasing in the reproduced wave field. For an even number of angular sampling positions this results in the following anti-aliasing condition

$$\mathring{D}(\nu, R, \omega) = \begin{cases} \mathring{D}(\nu, R, \omega) & \text{for } -\frac{N}{2} + 1 \leq \nu \leq \frac{N}{2}, \\ 0 & \text{otherwise.} \end{cases}$$

(17)

The anti-aliasing condition (17) poses limitations on the spatial structure of the desired wave field. Typically no such limitation is performed in practical implementations of reproduction systems. In the following the sampling artifacts for the reproduction of arbitrary wave fields that do not fulfill the anti-aliasing condition (17) are discussed.

The formulation of the reproduced wave field in terms of angular frequencies given by Eq. (16) is used to split the reproduced wave field $P_{\mathrm{P,S}}(\mathbf{x_P}, \omega)$ into the wave field $P_{\mathrm{P,S,0}}(\mathbf{x_P}, \omega)$ without aliasing contributions and into its aliasing contributions $P_{\mathrm{P,S,al}}(\mathbf{x_P}, \omega)$. The wave field $P_{\mathrm{P,S,0}}(\mathbf{x_P}, \omega)$ would

have been reproduced by a continuous secondary source distribution. It is given by Eq. (13) or by the summation term with $\eta = 0$ in Eq. (16). The aliasing contributions $P_{\mathrm{P,S,al}}(\mathbf{x_P}, \omega)$ reproduced by a discretized secondary source distribution are derived from the spectral repetitions present in Eq. (16) as

$$P_{\mathrm{P,S,al}}(\mathbf{x_P}, \omega) = -j\frac{\pi}{2}R \sum_{|\eta| \geq 1} \sum_{\nu=-\infty}^{\infty} \times$$
$$\times J_\nu(kr) H_\nu^{(2)}(kR) \mathring{D}_{\mathrm{S}}(\nu + \eta N, R, \omega) e^{j\nu\alpha} . \quad (18)$$

The split-up of the reproduced wave field is used to calculate the energy of the aliasing contributions with respect to the desired wave field. The reproduced aliasing-to-signal ratio RASR is defined as follows

$$\mathrm{RASR}(\mathbf{x_P}, \omega) = \frac{\int_0^\omega |P_{\mathrm{P,S,al}}(\mathbf{x_P}, \omega')|^2 \, d\omega'}{\int_0^\omega |P_{\mathrm{P,S,0}}(\mathbf{x_P}, \omega')|^2 \, d\omega'} . \quad (19)$$

In general, the RASR will depend on the desired wave field and the listener position. The RASR is zero for alias-free reproduction. In the following, the reproduction of a plane wave on a circular loudspeaker is considered.

4.2. Sampling artifacts for the reproduction of plane waves

The driving function for the reproduction of a plane wave is given according to Eq. (2) by considering the window function $a(\mathbf{x_0})$ and calculating the directional gradient of the wave field of a plane wave. The continuous driving function $D_{P,pw}(\alpha_0, R, \omega)$ for a plane wave is given as

$$
\begin{aligned}
D_{P,pw}(\alpha_0, R, \omega) = \\
= 2j\frac{\omega}{c}\, a(\alpha_0)\, \cos(\alpha_0 - \alpha_{pw})\, e^{-j\frac{\omega}{c}R\cos(\alpha_0 - \alpha_{pw})}\,,
\end{aligned}
\tag{20}
$$

where α_{pw} denotes the incidence angle of the plane wave. The window function $a(\alpha_0)$ for the circular array selects those secondary sources which are relevant for the reproduction of a plane wave with incidence angle α_{pw}. For the geometry depicted in Fig. 5 the window function is given as

$$
a_{pw}(\alpha_0) = \begin{cases} 1 & \text{for } \frac{\pi}{2} \le \alpha_0 - \alpha_{pw} \le \frac{3\pi}{2}, \\ 0 & \text{otherwise.} \end{cases}
\tag{21}
$$

Introducing Eq. (21) into Eq. (20) allows to calculate the Fourier series expansions coefficients $\mathring{D}_{S,pw}(\nu, R, \omega)$ of the sampled driving function for the reproduction of a plane wave. These can then be used to calculate the wave field reproduced by a discrete secondary source distribution using Eq. (16). The Jacobi-Anger expansion [22] states that a plane wave exhibits an infinite bandwidth in the angular frequency domain. As a result, no exact anti-aliasing condition can be given for the reproduction of plane waves on circular arrays. In the following results, the Fourier series coefficients $\mathring{D}_{S,pw}(\nu, R, \omega)$ of the sampled driving function for a plane wave were numerically calculated and introduced into Eq. (16).

4.3. Application Example

The reproduction of a band-limited (sinc-shaped) plane wave with an incidence angle of $\alpha_{pw} = \frac{3\pi}{2}$ on a circular array was evaluated as application example. The circular array consists of 48 secondary line sources placed on a circle with a radius of $R = 1.50$ m. The aliasing artifacts depend on the bandwidth of the desired plane wave. Figure 6(a) shows a snapshot of the reproduced wave field $P_{P,S}(\mathbf{x_P}, \omega)$ for a bandwidth of 1 kHz. The desired plane wave as well as the aliasing contributions can be clearly seen.

Figure 6(b) illustrates additionally the extracted aliasing contributions $P_{P,S,al}(\mathbf{x_P}, \omega)$ of Fig. 6(a). Figure 7 shows the $\text{RASR}(\mathbf{x_P}, \omega)$ for different maximum frequencies. The presented results show that the RASR is dependent on the listener position and the bandwidth of the reproduced plane wave. Two conclusions can be drawn from Fig. 7: (1) the higher the bandwidth of the plane wave is, the more energy is contained in the aliasing contributions of the reproduced field and (2) the farer the listener position is from the active secondary sources, the lower is the energy of the aliasing contributions. The latter conclusion was also derived for the truncated linear arrays discussed in Section 3.

The results shown in this section hold also for other incidence angles of the reproduced plane wave due to the symmetry of the circular secondary source contour. This implies that the minimum value of the RASR is reached in the center of the array for the reproduction of arbitrary wave fields with contributions from all sides.

5. POINT SOURCES AS SECONDARY SOURCES FOR SOUND REPRODUCTION

Typical implementations of two-dimensional sound reproduction and WFS systems utilize point sources (closed loudspeakers) instead of line sources as secondary sources. This section will briefly illustrate that the derived anti-aliasing conditions apply also to such reproduction systems. Without loss of generality this will be shown by the example of the linear secondary source distribution discussed in Section 3. Figure 3 illustrates the real part of the spectrum for the reproduction of a monochromatic plane wave using a discrete distribution of line sources. In this case the Dirac lines represent the sampled driving function and the circular Dirac function the real part of the spectrum of a line source. The wave field produced by a point source is given by the three-dimensional free-field Green's function $G_{3D}(\mathbf{x}|\mathbf{x}_0, \omega)$. The wave field $\tilde{P}_{C,S,pw,3D}(\mathbf{k}, \omega)$ reproduced by a spatially discrete linear distribution of secondary point sources is given by exchanging the two-dimensional Green's function $\tilde{G}_{2D}(\mathbf{k}, \omega)$ with its three-dimensional counterpart $\tilde{G}_{3D}(\mathbf{k}, \omega)$ and introducing the driving function for the reproduction of
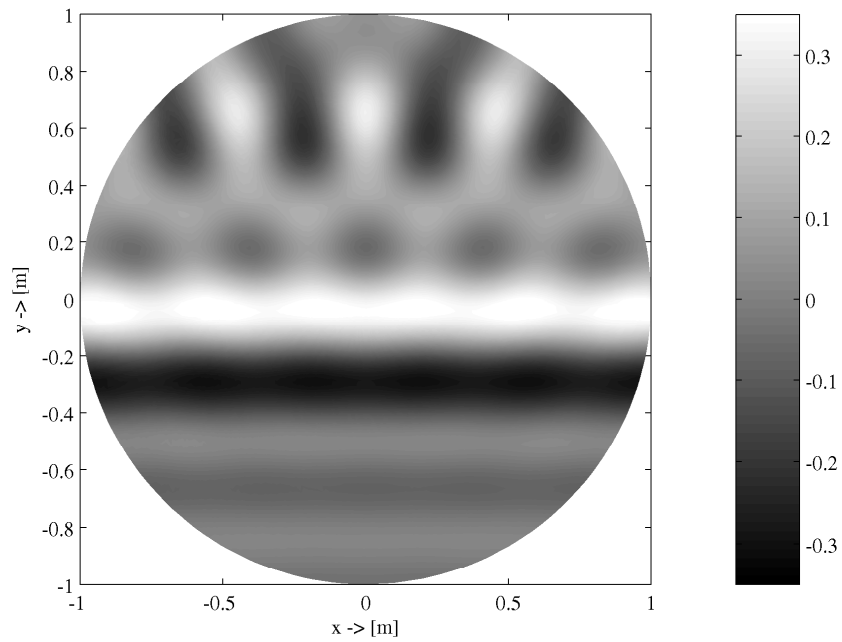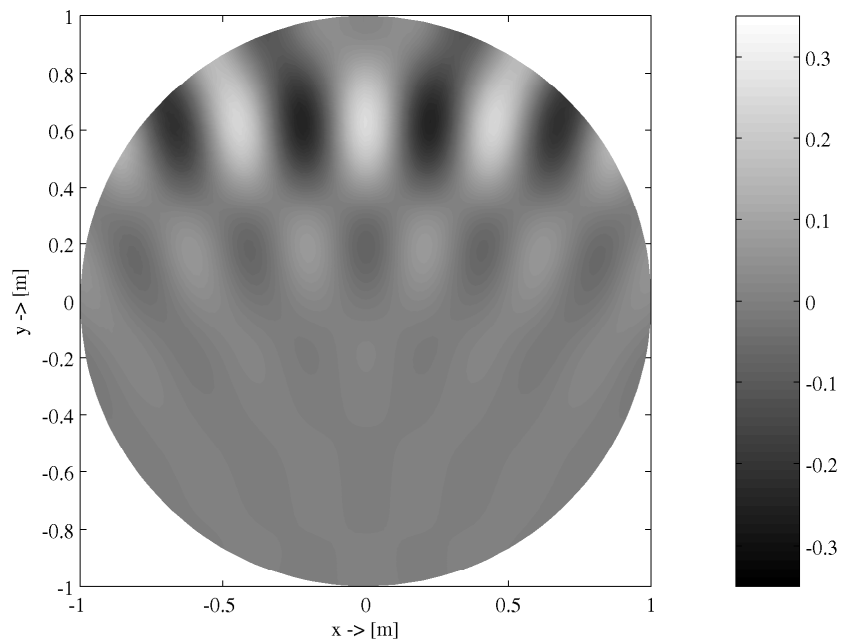
(a) reproduced wave field $P_{\mathrm{P,S}}(\mathbf{x}_{\mathrm{P}}, \omega)$

(b) aliasing contributions $P_{\mathrm{P,S,al}}(\mathbf{x}_{\mathrm{P}}, \omega)$

Fig. 6: Reproduction of a band-limited plane wave with $\alpha_{\mathrm{pw}} = \frac{3\pi}{2}$ on a array with $N = 48$ secondary sources and a radius of $R = 1.50$ m. The plane wave has a bandwidth of 1 kHz. The upper plot shows the reproduced wave field, the lower one its aliasing contributions.
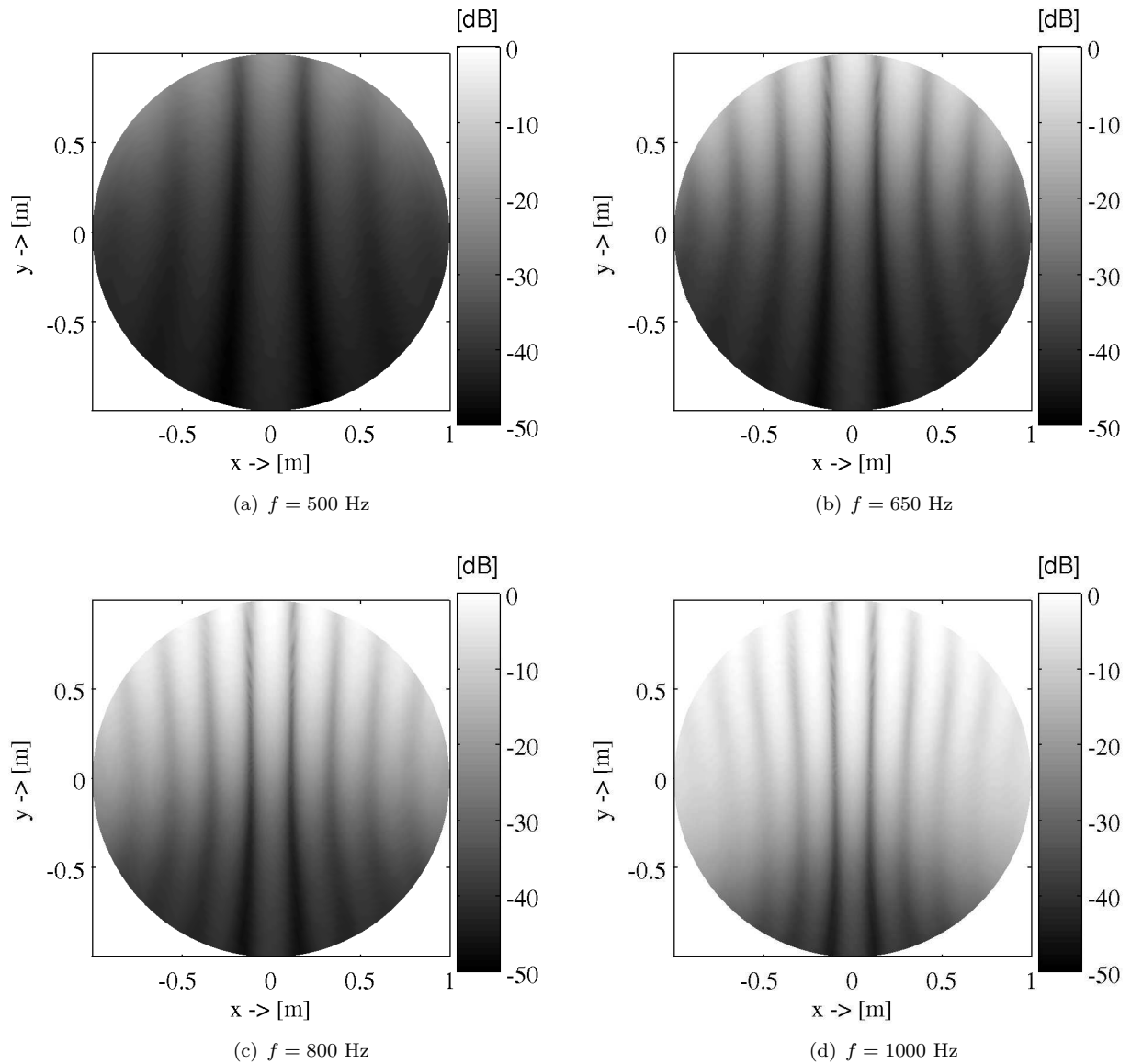
(a) $f = 500$ Hz

(b) $f = 650$ Hz

(c) $f = 800$ Hz

(d) $f = 1000$ Hz

Fig. 7: RASR($\mathbf{x}_\mathrm{P}, \omega$) for a circular array with $N = 48$ secondary sources and a radius of $R = 1.50$ m when reproducing a band-limited Dirac shaped plane wave. The gray levels denote the level in [dB].

a plane wave into Eq. (8)

$$\tilde{P}_{\mathrm{C},S,\mathrm{pw},\mathrm{3D}}(\mathbf{k},\omega) = \frac{\omega}{2\pi c}\sin\alpha_{\mathrm{pw}} \times$$

$$\sum_{\eta=-\infty}^{\infty}\delta(k_x - \frac{2\pi}{\Delta x}\eta - \frac{\omega}{c}\cos\alpha_{\mathrm{pw}})\underbrace{\frac{1}{\sqrt{(\frac{\omega}{c})^2 - k_x^2 - k_y^2}}}_{Q_{\mathrm{C}}(\mathbf{k}_{\mathrm{C}},\omega)} \; .$$

(22)

where $Q_{\mathrm{C}}(\mathbf{k}_{\mathrm{C}},\omega)$ abbreviates the contribution emerging from the spectrum of a secondary point source. The singular value of $Q_{\mathrm{C}}(\mathbf{k}_{\mathrm{C}},\omega)$ is located on a circle with radius $\frac{\omega}{c}$ in the spatial frequency domain as illustrated in Fig. 3. Inside of this circle $Q_{\mathrm{C}}(\mathbf{k}_{\mathrm{C}},\omega)$ is real and outside imaginary valued. Applying the sifting property of the Dirac line to this term yields that the reproduced spectrum is given by evaluating $Q_{\mathrm{C}}(\mathbf{k}_{\mathrm{C}},\omega)$ at $k_x = \frac{2\pi}{\Delta x}\eta + \frac{\omega}{c}\cos\alpha_{\mathrm{pw}}$. The propagating (non-evanescent) part of the reproduced wave field is then given by the resulting spectral contributions inside the circle depicted in Fig. 3. Hence, the anti-aliasing condition (10) derived for the reproduction of monochromatic plane waves by line sources as secondary sources applies also to the reproduction using point sources. The presented theory holds therefore also for WFS based reproduction systems. For the evanescent part condition (10) holds only approximately as for line sources as secondary sources. However, their significant contributions are restricted to the near-field of the secondary sources.

6. CONCLUSIONS

This paper presented a detailed analysis of the sampling artifacts produced by linear and circular loudspeaker arrays. This analysis was performed by deriving analytic expressions of the wave field reproduced by a spatially discrete secondary source distribution. This description in the spatial frequency domain allowed to isolate the spatial aliasing artifacts from the desired wave field. The main results of this analysis are: (1) on linear arrays spatial aliasing exhibits the form of tilted plane waves for the reproduction of monochromatic plane waves, (2) on truncated linear arrays the audibility of these tilted plane wave constituting aliasing depends on the listener position and (3) the reproduction of a plane wave on a circular array will always exhibit aliasing without

limitation of the angular bandwidth of the desired plane wave. The latter conclusion implies that every spatially discrete circular secondary source distribution will produce aliasing artifacts without modification of the virtual source wave field.

Spatial aliasing artifacts can be avoided for linear arrays by a limitation of the temporal bandwidth and/or the incidence angle of the reproduced plane wave. For circular arrays aliasing can be avoided by limiting the angular bandwidth of the virtual source wave field.

The presented analysis may be of use to describe the psychoacoustic effects that lead to a limited perception of spatial aliasing artifacts on the one side, and on the other side to quantify the limits of active control applications like active listening room compensation.

7. REFERENCES

[1] T. Ajdler, L. Sbaiz, and M. Vetterli, "Plenacoustic function on the circle with application to HRTF interpolation," in *IEEE International Conference on Acoustics, Speech, and Signal Processing (ICASSP)*, Philadephia, USA, 2005.

[2] J. Coleman, "Ping-pong sample times on a linear array halve the nyquist rate," in *IEEE International Conference on Acoustics, Speech, and Signal Processing (ICASSP)*, Montreal, Canada, 2004.

[3] W. de Bruin, *Application of Wave Field Synthesis in Videoconferencing*, Ph.D. thesis, Delft University of Technology, 2004.

[4] E.W. Start, *Direct Sound Enhancement by Wave Field Synthesis*, Ph.D. thesis, Delft University of Technology, 1997.

[5] H. Wittek, "Räumliche Wahrnehmung von Wellenfeldsynthese – Der Einfluss von Alias-Effekten auf die Klangfarbe," in *31. Deutsche Jahrestagung für Akustik*, Munic, Germany, 2005.

[6] S. Spors, H. Buchner, and R. Rabenstein, "Efficient active listening room compensation for Wave Field Synthesis," in *116th AES Convention*, Berlin, Germany, 2004, Audio Engineering Society (AES).

[7] D. Leckschat and M. Baumgartner, "Wellen-feldsynthese: Untersuchungen zu Alias-Artefakten im Ortsfrequenzbereich und Realisierung eines praxistauglichen WFS-Systems," in *31. Deutsche Jahrestagung für Akustik*, Munic, Germany, 2005.

[8] E.G. Williams, *Fourier Acoustics: Sound Radiation and Nearfield Acoustical Holography*, Academic Press, 1999.

[9] E.W. Start, "Application of curved arrays in wave field synthesis," in *110th AES Convention*, Copenhagen, Denmark, May 1996, Audio Engineering Society (AES).

[10] S. Spors, *Active Listening Room Compensation for Spatial Sound Reproduction Systems*, Ph.D. thesis, University of Erlangen-Nuremberg, 2006.

[11] R. Rabenstein and S. Spors, "Wave field synthesis techniques for spatial sound reproduction," in *Selected Methods of Acoustic Echo and Noise Control*, E.Haensler and G.Schmidt, Eds. Wiley, 2006, To be published.

[12] L.J. Ziomek, *Fundamentals of Acoustic Field Theory and Space Time Signal Processing*, CRC Press, 1995.

[13] M. Abramowitz and I.A. Stegun, *Handbook of Mathematical Functions*, Dover Publications, 1972.

[14] A.J. Berkhout, "A holographic approach to acoustic control," *Journal of the Audio Engineering Society*, vol. 36, pp. 977–995, December 1988.

[15] E.N.G. Verheijen, *Sound Reproduction by Wave Field Synthesis*, Ph.D. thesis, Delft University of Technology, 1997.

[16] P. Vogel, *Application of Wave Field Synthesis in Room Acoustics*, Ph.D. thesis, Delft University of Technology, 1993.

[17] D. de Vries, E.W. Start, and V.G. Valstar, "The Wave Field Synthesis concept applied to sound reinforcement: Restrictions and solutions," in *96th AES Convention*, Amsterdam, Netherlands, February 1994, Audio Engineering Society (AES).

[18] J.-J. Sonke, D. de Vries, and J. Labeeuw, "Variable acoustics by wave field synthesis: A closer look at amplitude effects," in *104th AES Convention*, Amsterdam, Netherlands, May 1998, Audio Engineering Society (AES).

[19] S. Spors, M. Renk, and R. Rabenstein, "Limiting effects of active room compensation using wave field synthesis," in *118th AES Convention*, Barcelona, Spain, May 2005, Audio Engineering Society (AES).

[20] S. Spors, "Spatial aliasing artifacts produced by linear loudspeaker arrays used for wave field synthesis," in *Second IEEE-EURASIP International Symposium on Control, Communications, and Signal Processing*, Marrakech, Morocco, March 2006.

[21] R.N. Bracewell, *The Fourier Transform and its Applications*, McGraw-Hill, 1978.

[22] I.S. Gradshteyn and I.M. Ryzhik, *Tables of Integrals, Series, and Products*, Academic Press, 2000.